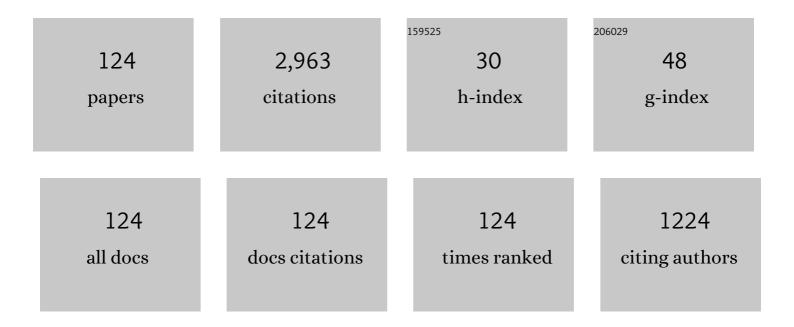
Huai-chun Zhou

List of Publications by Year in descending order

Source: https://exaly.com/author-pdf/9527279/publications.pdf Version: 2024-02-01



#	Article	IF	CITATIONS
1	Experimental investigations on visualization of three-dimensional temperature distributions in a large-scale pulverized-coal-fired boiler furnace. Proceedings of the Combustion Institute, 2005, 30, 1699-1706.	2.4	195
2	Numerical simulations of the slagging characteristics in a down-fired, pulverized-coal boiler furnace. Fuel Processing Technology, 2010, 91, 88-96.	3.7	127
3	Visualization of three-dimensional temperature distributions in a large-scale furnace via regularized reconstruction from radiative energy images: numerical studies. Journal of Quantitative Spectroscopy and Radiative Transfer, 2002, 72, 361-383.	1.1	121
4	Calculations of gas thermal radiation transfer in one-dimensional planar enclosure using LBL and SNB models. International Journal of Heat and Mass Transfer, 2011, 54, 4736-4745.	2.5	106
5	Deduction of the two-dimensional distribution of temperature in a cross section of a boiler furnace from images of flame radiation. Combustion and Flame, 2005, 143, 97-105.	2.8	95
6	Improving the Performance of a 300 MW Down-Fired Pulverized-Coal Utility Boiler by Inclining Downward the F-Layer Secondary Air. Energy & Fuels, 2010, 24, 4857-4865.	2.5	85
7	Measurements of the flame emissivity and radiative properties of particulate medium in pulverized-coal-fired boiler furnaces by image processing of visible radiation. Proceedings of the Combustion Institute, 2007, 31, 2771-2778.	2.4	69
8	A simple measurement method of temperature and emissivity of coal-fired flames from visible radiation image and its application in a CFB boiler furnace. Fuel, 2009, 88, 980-987.	3.4	68
9	A Combustion-Monitoring System With 3-D Temperature Reconstruction Based on Flame-Image Processing Technique. IEEE Transactions on Instrumentation and Measurement, 2007, 56, 1877-1882.	2.4	65
10	A simple judgment method of gray property of flames based on spectral analysis and the two-color method for measurements of temperatures and emissivity. Proceedings of the Combustion Institute, 2011, 33, 735-741.	2.4	65
11	Numerical Simulation of Multifuel Combustion in a 200 MW Tangentially Fired Utility Boiler. Energy & Fuels, 2012, 26, 313-323.	2.5	63
12	Experimental investigation on simultaneous measurement of temperature distributions and radiative properties in an oil-fired tunnel furnace by radiation analysis. International Journal of Heat and Mass Transfer, 2011, 54, 1-8.	2.5	62
13	Effects of total pressure on non-grey gas radiation transfer in oxy-fuel combustion using the LBL, SNB, SNBCK, WSGG, and FSCK methods. Journal of Quantitative Spectroscopy and Radiative Transfer, 2016, 172, 24-35.	1.1	60
14	Calculations of gas radiation heat transfer in a two-dimensional rectangular enclosure using the line-by-line approach and the statistical narrow-band correlated-k model. International Journal of Thermal Sciences, 2012, 59, 66-74.	2.6	55
15	Review of soot measurement in hydrocarbon-air flames. Science China Technological Sciences, 2010, 53, 2129-2141.	2.0	53
16	Experiments on Measurement of Temperature and Emissivity of Municipal Solid Waste (MSW) Combustion by Spectral Analysis and Image Processing in Visible Spectrum. Energy & Fuels, 2013, 27, 6754-6762.	2.5	52
17	A new way to calculate radiative intensity and solve radiative transfer equation through using the Monte Carlo method. Journal of Quantitative Spectroscopy and Radiative Transfer, 2004, 83, 459-481.	1.1	50
18	Measurement of Soot Temperature and Volume Fraction of Axisymmetric Ethylene Laminar Flames Using Hyperspectral Tomography. IEEE Transactions on Instrumentation and Measurement, 2017, 66, 315-324.	2.4	49

#	Article	IF	CITATIONS
19	Experiments investigation on 2D distribution of soot temperature and volume fraction by image processing of visible radiation. Applied Thermal Engineering, 2017, 124, 1014-1022.	3.0	48
20	Measurement of distributions of temperature and wavelength-dependent emissivity of a laminar diffusion flame using hyper-spectral imaging technique. Measurement Science and Technology, 2016, 27, 025201.	1.4	46
21	Simultaneous Measurement of Three-Dimensional Temperature Distributions and Radiative Properties Based on Radiation Image Processing Technology in a Gas-Fired Pilot Tubular Furnace. Heat Transfer Engineering, 2014, 35, 770-779.	1.2	45
22	The influence of anisotropic scattering on the radiative intensity in a gray, plane-parallel medium calculated by the DRESOR method. Journal of Quantitative Spectroscopy and Radiative Transfer, 2007, 104, 99-115.	1.1	43
23	Development of a distributed-parameter model for the evaporation system in a supercritical W-shaped boiler. Applied Thermal Engineering, 2014, 62, 123-132.	3.0	40
24	The effect of different HITRAN databases on the accuracy of the SNB and SNBCK calculations. International Journal of Heat and Mass Transfer, 2019, 129, 1232-1241.	2.5	37
25	Optimization of combustion based on introducing radiant energy signal in pulverized coal-fired boiler. Fuel Processing Technology, 2010, 91, 660-668.	3.7	34
26	Estimating soot volume fraction and temperature in flames using stochastic particle swarm optimization algorithm. International Journal of Heat and Mass Transfer, 2011, 54, 217-224.	2.5	34
27	Study on the surface active reactivity of coal char conversion in O2/CO2 and O2/N2 atmospheres. Fuel, 2016, 181, 1244-1256.	3.4	34
28	The DRESOR Method for a Collimated Irradiation on an Isotropically Scattering Layer. Journal of Heat Transfer, 2007, 129, 634-645.	1.2	32
29	Principles of optimization of combustion by radiant energy signal and its application in a 660 MWe down- and coal-fired boiler. Korean Journal of Chemical Engineering, 2011, 28, 2336-2343.	1.2	31
30	Investigation on the ignition, thermal acceleration and characteristic temperatures of coal char combustion. Applied Thermal Engineering, 2017, 113, 1303-1312.	3.0	31
31	Measurements on flame temperature and its 3D distribution in a 660 MWe arch-fired coal combustion furnace by visible image processing and verification by using an infrared pyrometer. Measurement Science and Technology, 2009, 20, 114006.	1.4	29
32	Estimation of radiative properties and temperature distributions in coal-fired boiler furnaces by a portable image processing system. Experimental Thermal and Fluid Science, 2011, 35, 416-421.	1.5	28
33	The DRESOR method for transient radiation transfer in 1-D graded index medium with pulse irradiation. International Journal of Thermal Sciences, 2013, 68, 127-135.	2.6	28
34	An inverse radiative transfer problem of simultaneously estimating profiles of temperature and radiative parameters from boundary intensity and temperature measurements. Journal of Quantitative Spectroscopy and Radiative Transfer, 2002, 74, 605-620.	1.1	27
35	Experimental study on acoustic vector tomography of 2-D flow field in an experiment-scale furnace. Flow Measurement and Instrumentation, 2006, 17, 113-122.	1.0	27
36	An improved colorimetric method for visualization of 2-D, inhomogeneous temperature distribution in a gas fired industrial furnace by radiation image processing. Proceedings of the Combustion Institute, 2011, 33, 2755-2762.	2.4	27

#	Article	IF	CITATIONS
37	Mathematical modeling and experimental validation of ash deposition in a pulverized-coal boiler. Applied Thermal Engineering, 2017, 110, 720-729.	3.0	27
38	Silicon complex grating with different groove depths as an absorber for solar cells. Journal of Quantitative Spectroscopy and Radiative Transfer, 2014, 132, 70-79.	1.1	26
39	A NEW MODEL OF RADIATIVE IMAGE FORMATION USED IN VISUALIZATION OF 3-D TEMPERATURE DISTRIBUTIONS IN LARGE-SCALE FURNACES. Numerical Heat Transfer, Part B: Fundamentals, 2002, 42, 243-258.	0.6	25
40	Implementation of tridirectional large lateral shearing displacement interferometry in temperature measurement of a diffused ethylene flame. Applied Optics, 2011, 50, 3924.	2.1	25
41	Simultaneous reconstruction of temperature distribution, absorptivity of wall surface and absorption coefficient of medium in a 2-D furnace system. International Journal of Heat and Mass Transfer, 2003, 46, 2645-2653.	2.5	24
42	The Solution of Transient Radiative Transfer With Collimated Incident Serial Pulse in a Plane-Parallel Medium by the DRESOR Method. Journal of Heat Transfer, 2008, 130, .	1.2	23
43	Char burnout characteristics of five coals below and above ash flow temperature: TG, SEM, and EDS analysis. Applied Thermal Engineering, 2016, 103, 1156-1163.	3.0	23
44	Simultaneous estimation of the profiles of the temperature and the scattering albedo in an absorbing, emitting, and isotropically scattering medium by inverse analysis. International Journal of Heat and Mass Transfer, 2000, 43, 4361-4364.	2.5	21
45	Simultaneous Determination of Distributions of Temperature and Soot Volume Fraction in Sooting Flames Using Decoupled Reconstruction Method. Numerical Heat Transfer; Part A: Applications, 2009, 56, 153-169.	1.2	21
46	Modeling of ash deposition in a pulverized-coal boiler by direct simulation Monte Carlo method. Fuel, 2016, 184, 604-612.	3.4	21
47	Experimental investigation on gas-phase temperature of axisymmetric ethylene flames by large lateral shearing interferometry. International Journal of Thermal Sciences, 2017, 115, 104-111.	2.6	21
48	Study on the combustion behavior and soot formation of single coal particle using hyperspectral imaging technique. Combustion and Flame, 2021, 233, 111568.	2.8	21
49	The DRESOR method for one-dimensional transient radiative transfer in graded index medium coupled with BRDF surface. International Journal of Thermal Sciences, 2015, 91, 96-104.	2.6	20
50	Measurement of the distribution of temperature and emissivity of a candle flame using hyperspectral imaging technique. Optik, 2019, 183, 222-231.	1.4	20
51	The impact of combustion characteristics and flame structure on soot formation in oxy-enhanced and oxy-fuel diffusion flames. Science China Technological Sciences, 2013, 56, 1618-1628.	2.0	19
52	Non-imaging concentrating reflectors designed for solar concentration systems. Solar Energy, 2014, 103, 494-501.	2.9	19
53	The DRESOR method for radiative heat transfer in a one-dimensional medium with variable refractive index. Journal of Quantitative Spectroscopy and Radiative Transfer, 2011, 112, 2835-2845.	1.1	18
54	Decoupled Reconstruction Method for Simultaneous Estimation of Temperatures and Radiative Properties in a One-Dimensional, Gray, Participating Medium. Numerical Heat Transfer, Part B: Fundamentals, 2007, 51, 275-292.	0.6	17

#	Article	IF	CITATIONS
55	The DRESOR method for radiative heat transfer in semitransparent graded index cylindrical medium. Journal of Quantitative Spectroscopy and Radiative Transfer, 2014, 143, 16-24.	1.1	17
56	Modeling of heat transfer and pyrolysis reactions in ethylene cracking furnace based on 3-D combustion monitoring. International Journal of Thermal Sciences, 2015, 94, 28-36.	2.6	17
57	Flexibility of a 300 MW Arch Firing Boiler Burning Low Quality Coals. Mining Science and Technology, 2007, 17, 566-571.	0.8	16
58	Distributed parameter modeling and simulation for the evaporation system of a controlled circulation boiler based on 3-D combustion monitoring. Applied Thermal Engineering, 2008, 28, 164-177.	3.0	16
59	Assessment of Regularized Reconstruction of Three-Dimensional Temperature Distributions in Large-Scale Furnaces. Numerical Heat Transfer, Part B: Fundamentals, 2008, 53, 555-567.	0.6	16
60	Distributed parameters modeling for evaporation system in a once-through coal-fired twin-furnace boiler. International Journal of Thermal Sciences, 2011, 50, 2496-2505.	2.6	16
61	Improved Discrete Ordinates Method for Ray Effects Mitigation. Journal of Heat Transfer, 2011, 133, .	1.2	16
62	Highly-Directional Radiative Intensity in a 2-D Rectangular Enclosure Calculated by the DRESOR Method. Numerical Heat Transfer, Part B: Fundamentals, 2008, 54, 354-367.	0.6	15
63	Spatial and temporal film thickness measurement of a soap bubble based on large lateral shearing displacement interferometry. Applied Optics, 2012, 51, 8863.	0.9	15
64	Temperature measurement by holographic interferometry for non-premixed ethylene-air flame with a series of state relationships. Fuel, 2007, 86, 1552-1559.	3.4	14
65	Calculations of narrow-band transimissities and the Planck mean absorption coefficients of real gases using line-by-line and statistical narrow-band models. Frontiers in Energy, 2014, 8, 41-48.	1.2	14
66	A new method for constructing radiative energy signal in a coal-fired boiler. Applied Thermal Engineering, 2016, 101, 446-454.	3.0	14
67	Quantitative evaluation of the computational accuracy for the Monte Carlo calculation of radiative heat transfer. Journal of Quantitative Spectroscopy and Radiative Transfer, 2019, 226, 100-114.	1.1	14
68	An improved full-spectrum correlated-k-distribution model for non-gray radiative heat transfer in combustion gas mixtures. International Communications in Heat and Mass Transfer, 2020, 114, 104566.	2.9	14
69	The effect of BRDF surface on radiative heat transfer within a one-dimensional graded index medium. International Journal of Thermal Sciences, 2014, 77, 116-125.	2.6	13
70	Effects of radiation reabsorption of C1-C6 hydrocarbon flames at normal and elevated pressures. Fuel, 2020, 266, 117061.	3.4	13
71	THE DRESOR METHOD FOR THE SOLUTION OF THE RADIATIVE TRANSFER EQUATION IN GRAY PLANE-PARALLEL MEDIA. , 2004, , .		13
72	Equation-solving DRESOR method for radiative transfer in a plane-parallel, absorbing, emitting, and isotropically scattering medium with transparent boundaries. International Journal of Heat and Mass Transfer, 2012, 55, 3454-3457.	2.5	12

#	Article	IF	CITATIONS
73	Spatial and temporal thermal analysis of acousto-optic deflectors using finite element analysis model. Ultrasonics, 2012, 52, 643-649.	2.1	12
74	Simulation on simultaneous estimation of non-uniform temperature and soot volume fraction distributions in axisymmetric sooting flames. Journal of Quantitative Spectroscopy and Radiative Transfer, 2005, 91, 11-26.	1.1	11
75	Solution of radiative intensity with high directional resolution in three-dimensional rectangular enclosures by DRESOR method. International Journal of Heat and Mass Transfer, 2013, 60, 81-87.	2.5	11
76	Visualization of 3-D temperature distribution in a 300 MW twin-furnace coal-fired boiler. Mining Science and Technology, 2008, 18, 33-37.	0.8	10
77	Existence of Dual-Peak Temporal Reflectance from a Light Pulse Irradiated Two-Layer Medium. Numerical Heat Transfer; Part A: Applications, 2009, 56, 342-359.	1.2	10
78	Recent achievements in measurements of soot volume fraction and temperatures in a coflow, diffuse Ethylene-air flame by visible image processing. Journal of Physics: Conference Series, 2009, 147, 012086.	0.3	10
79	Modeling of Soot Formation in Gas Burner Using Reduced Chemical Kinetics Coupled with CFD Code. Chinese Journal of Chemical Engineering, 2010, 18, 967-978.	1.7	10
80	Calculations of thermal radiation transfer of C2H2 and C2H4 together with H2O, CO2, and CO in a one-dimensional enclosure using LBL and SNB models. Journal of Quantitative Spectroscopy and Radiative Transfer, 2017, 197, 45-50.	1.1	10
81	A decomposition method for the simultaneous reconstruction of temperature and soot volume fraction distributions in axisymmetric flames. Measurement Science and Technology, 2020, 31, 115202.	1.4	10
82	Experimental investigations of temperature distribution in non-premixed flames with different gas compositions by large lateral shearing interferometry. Journal of Quantitative Spectroscopy and Radiative Transfer, 2019, 224, 445-452.	1.1	9
83	Quasi-constant temperature combustion for improving the overall performance of a coal-fired boiler. Combustion and Flame, 2003, 134, 81-92.	2.8	8
84	Solution of radiative transfer in a oneâ€dimensional anisotropic scattering media with different boundary conditions using the DRESOR method. Heat Transfer - Asian Research, 2008, 37, 138-152.	2.8	8
85	Experimental detection of radiative energy signal from a supercharged marine boiler and simulation on its application in control of drum water level. Applied Thermal Engineering, 2011, 31, 3168-3175.	3.0	8
86	Study on the measurement of temperature field using laser holographic interferometry. Frontiers in Energy, 2011, 5, 120-124.	1.2	8
87	Acoustic reconstruction of the velocity field in a furnace using a characteristic flow model. Journal of the Acoustical Society of America, 2012, 131, 4399-4408.	0.5	8
88	Performance comparison of two monte carlo ray-tracing methods for calculating radiative heat transfer. Journal of Quantitative Spectroscopy and Radiative Transfer, 2020, 256, 107305.	1.1	8
89	Simultaneous Determination of Na Concentration and Temperature during Zhundong Coal Combustion using the Radiation Spectrum. Energy & amp; Fuels, 2021, 35, 3348-3359.	2.5	8
90	The Iterative-DRESOR method to solve radiative transfer in a plane-parallel, anisotropic scattering medium with specular-diffuse boundaries. Journal of Quantitative Spectroscopy and Radiative Transfer, 2009, 110, 1072-1084.	1.1	7

#	Article	IF	CITATIONS
91	Computation and measurement for distributions of temperature and soot volume fraction in diffusion flames. Central South University, 2011, 18, 1263-1271.	0.5	7
92	Effect of radiative transfer of heat released from combustion reaction on temperature distribution: A numerical study for a 2-D system. Journal of Quantitative Spectroscopy and Radiative Transfer, 2006, 101, 109-118.	1.1	6
93	SCT reaction kinetics model and diffusion for p.c. combustion in TGA. Asia-Pacific Journal of Chemical Engineering, 2010, 5, 390-395.	0.8	6
94	Road surface mirage: A bunch of hot air?. Science Bulletin, 2011, 56, 962-968.	1.7	6
95	Effects of surface emissivity and medium scattering albedo on the computational accuracy of radiative heat transfer by MCM. Journal of Quantitative Spectroscopy and Radiative Transfer, 2020, 240, 106712.	1.1	6
96	A wavelet model on reconstructing complex aerodynamic field in furnace with acoustic tomography. Measurement: Journal of the International Measurement Confederation, 2020, 157, 107669.	2.5	6
97	Distributed parameter modeling and thermal analysis of a spiral water wall in a supercritical boiler. Thermal Science, 2013, 17, 1337-1342.	0.5	5
98	The effect of non-linear interaction between gas and particle velocities on the hydrodynamic stability in the Blasius boundary layer. International Journal of Non-Linear Mechanics, 2009, 44, 106-114.	1.4	4
99	A compact optimization strategy for combustion in a 125 MW tangentially anthracite-fired boiler by an artificial neural network. Asia-Pacific Journal of Chemical Engineering, 2008, 3, 432-439.	0.8	3
100	Nongray radiation from gas and soot mixtures in planar plates based on statistical narrow-band spectral model. Frontiers in Energy, 2011, 5, 149-158.	1.2	3
101	A Hybrid Partial Coherence and Geometry Optics Model of Radiative Property on Coated Rough Surfaces. Journal of Heat Transfer, 2013, 135, .	1.2	3
102	Finite-difference time-domain modeling of curved material interfaces by using boundary condition equations method. Chinese Physics B, 2016, 25, 090203.	0.7	3
103	Key parameter analysis of the DRESOR method for calculating the radiative heat transfer in three-dimensional absorbing, emitting and scattering media. International Journal of Thermal Sciences, 2021, 168, 107047.	2.6	3
104	Numerical reproduction and explanation of road surface mirages under grazing-angle scattering. Applied Optics, 2017, 56, 5550.	0.9	3
105	Activation of the calciumâ€added coal combustion solid residues. Asia-Pacific Journal of Chemical Engineering, 2007, 2, 177-181.	0.8	2
106	Thickness measurement of full field soap bubble film in real time based on large lateral shearing displacement interferometry. , 2012, , .		2
107	Equation Solving DRESOR Method for Radiative Transfer in Three-Dimensional Isotropically Scattering Media. Journal of Heat Transfer, 2014, 136, .	1.2	2
108	The Phenomena of Secondary Weight Loss in High-Temperature Coal Pyrolysis. Energy & Fuels, 2017, 31, 10178-10185.	2.5	2

#	Article	IF	CITATIONS
109	Determination of the binary gas diffusion coefficients using large lateral shearing interferometry. Optik, 2018, 156, 825-833.	1.4	2
110	Combustion Stability Assessment for Utility Pulverized Coal-Fired Boilers under Low Loads. Combustion Science and Technology, 2000, 157, 325-340.	1.2	1
111	Fabrication of independent virtual lines for reconstruction of 2D source distribution with high spatial resolution equal to that of limited projections. , 2013, , .		1
112	Optimization of the DRESOR method for application in a medium with large scattering albedo. Journal of Quantitative Spectroscopy and Radiative Transfer, 2021, 271, 107746.	1.1	1
113	Experimental and Simulation Investigations of Combustion Optimization on a 125 MW Tangentially Anthracite-fired Boiler. , 2007, , 644-651.		1
114	RES Induced for Combustion Optimized Control and Low NO x Emission in Thermal Power Generating Units. , 2007, , 620-623.		1
115	Numerical Simultaneous Determination of Non-Uniform Soot Temperature and Volume Fraction from Visible Flame Images. Energies, 2022, 15, 2770.	1.6	1
116	<title>Application of CCD images and colorimetry temperature measure for combustion monitoring and control</title> . , 2000, , .		0
117	Image processing applied to laser holographic interference fringes. , 2010, , .		0
118	Recontruction of temperature measurement for flame using holographic interferometry. , 2010, , .		0
119	Analysis of the Hydraulic Resistance of a Water Wall Based on a Distributed Parameter Model in a Supercritical Once-Through Boiler. Journal of Thermal Science and Engineering Applications, 2014, 6, .	0.8	0
120	An iterative virtual projection method to improve the reconstruction performance for ill-posed emission tomographic problems. Chinese Physics B, 2015, 24, 104204.	0.7	0
121	Real-time measurement method for the skin temperature of the human arm via large lateral shearing interferometry. Applied Optics, 2021, 60, 763.	0.9	0
122	A Hybrid Partial Coherence and Geometry Optics Model of Thin Film Optics on Coated Rough Surfaces. , 2012, , .		0
123	THE DRESOR METHOD FOR RADIATIVE HEAT TRANSFER IN A SEMITRANSPARENT GRADIENT INDEX CYLINDRICAL MEDIUM. , 2013, , .		0
124	Quantitative comparison of the DRESOR and Monte Carlo methods for calculating radiative heat flux. Numerical Heat Transfer; Part A: Applications, 0, , 1-18.	1.2	0